AGU PUBLICATIONS

JGR

Journal of Geophysical Research: Space Physics

RESEARCH ARTICLE
10.1002/2015JA021811

Key Points:
- Spatiospectral concentration is applied to VTEC estimating in Arctic region
- This research intends to improve accuracy of SH-based GIMs
- This theory can improve these ionospheric models up to 1 to 2 TECU in the Arctic region

Correspondence to:
H. Etemadfard,
hossein_etemadfard@yahoo.com;
hetemadfard@mail.kntu.ac.ir

Citation:
Etemadfard, H., and M. M. Hossainali (2016), Application of Slepian theory for improving the accuracy of SH-based global ionosphere models in the Arctic region, *J. Geophys. Res. Space Physics*, *120*, 2583-2594, doi:10.1002/2015JA021811.

Received 15 AUG 2015
Accepted 9 NOV 2015
Accepted article online 10 NOV 2015
Published online 14 MAR 2016

Application of Slepian theory for improving the accuracy of SH-based global ionosphere models in the Arctic region

Hossein Etemadfard[1] and Masoud Mashhadi Hossainali[1]

[1]Faculty of Geodesy and Geomatics Engineering, K. N. Toosi University of Technology, Tehran, Iran

Abstract Due to significant energy resources in polar regions, they have emerged as strategic parts of the world. Consequently, various researches have been funded in order to study these areas in further details. This research intends to improve the accuracy of spherical harmonic (SH)-based Global Ionospheric Models (GIMs) by reconstructing a new map of ionosphere in the Arctic region. For this purpose, the spatiospectral concentration is applied to optimize the base functions. It is carried out using the Slepian theory which was developed by Simons. Here the new base functions and the corresponding coefficients are derived from the SH models for the polar regions. Then, VTEC (vertical total electron content) is reconstructed using Slepian functions and the new coefficients. Reconstructed VTECs and the VTECs derived from SH models are compared to the estimates of this parameter, which are directly derived from dual-frequency GPS measurements. Three International Global Navigation Satellite Systems Service stations located in the northern polar region have been used for this purpose. The starting and ending day of year of adopted GPS data are 69 and 83, respectively, (totally 15 successive days) of the year 2013. According to the obtained results, on average, application of Slepian theory can improve accuracy of the GIM by 1 to 2 total electron content unit (TECU) (1 TECU = 10^{16} el m^{-2}) in the Arctic region.

1. Introduction

Day by day, poles are considered as a strategic part of the world due to the existing significant energy resources [*Liu et al.*, 2011]. For this reason, various researches are addressing these study areas including the physics of the atmosphere [*Aarons*, 1982, 1993; *Rodger and Graham*, 1996; *Skone*, 1998; *Basu et al.*, 2002; *Kunitsyn and Tereshchenko*, 2003; *Hunsucker and Hargreaves*, 2003; *Skone et al.*, 2005]. Aurorae and ionospheric irregularities and scintillations are two important atmospheric phenomena in the polar region [*Werink et al.*, 2003]. The analyzing impact of solar activities in ionosphere is a valuable information source of these phenomena [Fremouw *and Secan*, 1984; *Luhr and Xiong*, 2010] as well magnetic poles positions [*Skone*, 1998]. Moreover, ionosphere is one of the most important bias sources of Global Navigation Satellite Systems (GNSS) [*Parkinson and Spilker*, 1996; *Seeber*, 2003]. Hence, the GNSS signals are now currently used for remotely sensing of the Earth's atmosphere [*Skone*, 2009; *Jin et al.*, 2014].

So far, several models have been developed for estimation and prediction of ionosphere. They are usually classified as grid-based and function-based models [*Liu et al.*, 2011]. Ionosphere Exchange (IONEX) observation files as Global Ionospheric Models (GIMs) [*Schaer et al.*, 1998] and ionospheric products of Satellite-Based Augmentation System as a regional ionospheric model [*Liu et al.*, 2011] are two famous models of the first group. Klobuchar model, whose coefficients are transmitted by the GPS signals [*Klobuchar*, 1987], the polynomial model developed by *Komjathy* [1997], and the trigonometric series model of *Georgiadiou* [1994] are some examples for the latter models. Readers are referred to *Liu et al.*, [2008] for further details. Spherical cap harmonic (SCH) model is the most famous one for ionospheric modeling in the Arctic region [*Liu et al.*, 2011]. Another research utilized this method to map the Arctic total electron content (TEC) for the most recent solar cycle from 2000 to 2013. This research also analyzed the distributions and variations of the Arctic TEC at different temporal and spatial scales [*Liu et al.*, 2014a, 2014b]. SCH method is also developed to predict Arctic mean TEC on the scale of a solar cycle using previous data covering 14 years [*Liu et al.*, 2014a, 2014b].

GIMs provided by the International GNSS Service (IGS) have a temporal resolution of 2 h [*Dow et al.*, 2009]. More recently, IGS associated analysis centers are producing GIMs with time resolutions of 1 h to even

15 min [*García-Rigo et al*., 2014]. The total electron content (TEC) in zenith direction (VTEC, vertical TEC) is the parameter which is modeled by IGS center. GIMs are usually delivered in IONEX format. They are also provided in terms of spherical harmonic (SH) coefficients to the degree and order of both 15. In the production of GIMs, ionosphere is represented by a single layer [*Schaer*, 1999].

It is already known that the performance of these models in polar regions is poor [*Liu et al*., 2011]. It has been clearly expressed, for example, in the header part of the Klobuchar data file model. This poor performance is due to the complex impact of the solar activities and the geomagnetic field. In addition, conventional ionosphere models which are based on geodetic coordinates have an asynchronous dimensional resolution, especially in areas close to the pole [*Liu et al*., 2011]. Such problems have prompted researchers to develop new models tailored to these areas [*GhoddousiFard et al*., 2011; *Liu et al*., 2011].

This research intends to improve accuracy of GIMs based on SH in the Arctic region. For this purpose, spatiospectral concentration is applied on the SH models in order to optimize their base functions and also the corresponding coefficients. It is carried out using the Slepian theory [*Slepian and Pollak*, 1961; *Slepian*, 1976]. This theory has been extended to the sphere for bandlimited functions in the SHs domain by *Simons et al*. [2006].

The next section of this paper introduces SH approach for modeling ionosphere and discusses on the proposed method of this research. Then, the concept of model space resolution matrix is used for supporting the proposed approach and the corresponding results. Section 3 is allocated to the implementation of these methods and the comparison of the obtained results using the direct estimates of the vertical TEC.

2. VTEC Models

Modification and analysis of SHs (as the base functions) and estimating the coefficients of the modified base functions by the IGS SH coefficients are the main aims of this research. At the beginning, SH models are introduced. The method of this research for improving the accuracy of the IGS SH-based GIMs is given next. Finally, the theoretical background of the method which is used for analyzing and supporting the obtained results is discussed.

2.1. SH Model

SH modeling is a function-based approach to model the VTEC. The corresponding model is a combination of the Fourier series and the Legendre functions. SH functions are orthogonal on the surface of sphere. This property suggests SHs as appropriate base functions for modeling ionosphere in a global scale. The mathematical definition of VTEC in terms of these functions is as follows [*Schaer*, 1999]:

$$\mathrm{VTEC}(\theta_{\mathrm{IPP}},\xi_{\mathrm{IPP}}) = \sum_{l=0}^{K}\sum_{m=-l}^{l} \psi_{lm}\, Y_{lm}(\theta_{\mathrm{IPP}},\xi_{\mathrm{IPP}}), \tag{1}$$

where

θ_{IPP} geomagnetic colatitude of the ionospheric pierce point (IPP), degree;
ξ_{IPP} longitude of the IPP, degree;
l degree of SHs;
m order of SHs;
K maximum degree of SHs;
ψ_{lm} SH coefficients; and
Y_{lm} SH base functions.

SH base functions are defined as equation (2),

$$Y_{lm}(\theta_{\mathrm{IPP}},\xi_{\mathrm{IPP}}) = \begin{cases} \sqrt{2}X_{lm}(\theta_{\mathrm{IPP}})cos(m\xi_{\mathrm{IPP}}) \; if \; 0 < m \le l \\ X_{l0}(\theta_{\mathrm{IPP}}) \qquad if \; m = 0 \\ \sqrt{2}X_{lm}(\theta_{\mathrm{IPP}})\sin(m\xi_{\mathrm{IPP}}) \; if \; -l \le m < 0 \end{cases} \tag{2}$$

$$X_{lm}(\theta_{\mathrm{IPP}}) = (-1)^m \left(\frac{2l+1}{4\pi}\right)^{1/2} \left[\frac{(l-m)!}{(l+m)!}\right]^{1/2} P_{lm}(cos\theta_{\mathrm{IPP}})$$

$$P_{lm}(\mu) = \frac{1}{2^l l!}\left(1-\mu^2\right)^{m/2}\left(\frac{\mathrm{d}}{\mathrm{d}\mu}\right)^{l+m}(1-\mu)^l,$$

where P_{lm} is the Legendre function.

Moreover, the radial term is not presented in equation (1) because all of the VTEC parameters are assumed to be on a thin spherical shell at a specific height from the surface of the Earth. The degree and order of the Legendre functions define the resolution of a SH model.

2.2. Slepian-Based Function Approach

Spatiospectral concentration theory concerns the optimal space localization (time limitation) of a bandlimited signal in the frequency domain. The question was first considered by *Slepian and Pollak* [1961] and *Landau and Pollak* [1961, 1962] who studied the problem in one dimension. An introduction of a recent concerning this subject is provided by *Slepian* [1978, 1983]. Later, *Simons et al*. [2006, 2009] and *Simons* [2010] extended these results to the sphere for the bandlimited functions in the SH domain.

The orthogonality of SHs on the unit sphere, i.e., the thin spherical ionospheric shell, can be mathematically described as below,

$$\int_{\Omega} Y_{lm}(\theta_{\mathrm{IPP}},\xi_{\mathrm{IPP}})Y_{l'm'}(\theta_{\mathrm{IPP}},\xi_{\mathrm{IPP}})\mathrm{d}\Omega = \delta_{ll'}\delta_{mm'}, \tag{3}$$

where δ is the Kronecker's delta and Ω is the unit sphere.

Since equation (3) is not valid on an arbitrary region of unit sphere, R, application of SHs as the base functions of the model distorts the concentrated signal in the region. Orthogonalization of SHs on a region or, equivalently, optimization of the concentrated signals is a problem that can be solved by the Slepian theory. According to this theory, spatial concentration of the bandlimited function VTEC($\theta_{\mathrm{IPP}},\xi_{\mathrm{IPP}}$) is maximized in R by

$$\lambda = \frac{\|\mathrm{VTEC}(\theta_{\mathrm{IPP}},\xi_{\mathrm{IPP}})\|_R^2}{\|\mathrm{VTEC}(\theta_{\mathrm{IPP}},\xi_{\mathrm{IPP}})\|_{\Omega}^2} = \frac{\int_R \mathrm{VTEC}^2(\theta_{\mathrm{IPP}},\xi_{\mathrm{IPP}})d\Omega}{\int_{\Omega}\mathrm{VTEC}^2(\theta_{\mathrm{IPP}},\xi_{\mathrm{IPP}})d\Omega} = \max \tag{4}$$

Substituting equation (1) in equation (4),

$$\lambda = \frac{\sum_{l=0}^{K}\sum_{m=-l}^{l}\psi_{lm}\sum_{l'=0}^{K}\sum_{m'=-l'}^{l'}D_{lm,l'm'}\psi_{l'm'}}{\sum_{l=0}^{K}\sum_{m=-l}^{l}\psi_{lm}^2} \tag{5}$$

in which

$$D_{lm,l'm'} = \int_R Y_{lm}(\theta_{\mathrm{IPP}},\xi_{\mathrm{IPP}})\,Y_{l'm'}(\theta_{\mathrm{IPP}},\xi_{\mathrm{IPP}})\,\mathrm{d}\Omega \tag{6}$$

are the elements of the matrix $\mathbf{D}_{lm,l'm'}$ with dimensions $(l+1)^2\times(l+1)^2$. The spectral domain eigenvalue problem is used for computing the block diagonal matrix $\mathbf{D}=\mathrm{diag}\{\mathbf{D}^0,\mathbf{D}^1,\mathbf{D}^1,\ldots,\mathbf{D}^K,\mathbf{D}^K\}$. In this work, $\mathbf{D}^0=\mathbf{D}_{l0,l'0}=\mathbf{D}^0_{ll'}$, $\mathbf{D}^1=\mathbf{D}_{l1,l'1}=\mathbf{D}^1_{ll'}$, etc. Then, a simple analytical expression for equation (6) on the polar cap is derived when the order (m) is fixed,

$$D^m_{ll'} = (-1)^m\sqrt{\frac{(2l+1)(2l'+1)}{2}}\sum_{n=|l-l'|}^{l+l'}\begin{pmatrix} l & n & l' \\ 0 & 0 & 0\end{pmatrix}\begin{pmatrix} l & n & l' \\ m & 0 & -m\end{pmatrix}[P_{n-1}(\cos\theta_{\mathrm{IPP}})-P_{n+1}(\cos\theta_{\mathrm{IPP}})]. \tag{7}$$

In this work, the arrays of indices are the Wigner $3-j$ symbols [*Edmonds*, 1996; *Messiah*, 2000]. The next step would be the spectral decomposition of $\mathbf{D}^m$. It is elaborated using the equation below,

$$\mathbf{D}^m\mathbf{a}^m_l = \lambda^m_l\mathbf{a}^m_l \mathrm{or} \mathbf{D}^m\mathbf{A}^m = \mathbf{A}^m\mathbf{\Lambda}^m \tag{8}$$

where λ^m_l is the eigenvalue for the degree l and the order m and $\mathbf{a}^m_l$ is the orthonormal eigenvector corresponding to the eigenvalue.

Matrix of eigenvectors, $\mathbf{A}^m$, is used for the computation of Slepian functions from SHs. This leads to the equivalent of the prolate spheroidal wave functions on the sphere, as follows:

$$S^m_{\alpha}(\theta_{\mathrm{IPP}},\xi_{\mathrm{IPP}}) = \sum_{l=|m|}^{K}\left(\mathbf{a}^m_l\right)^T Y_{lm}(\theta_{\mathrm{IPP}},\xi_{\mathrm{IPP}}) \quad , \{|m|\le\alpha\le K\} \tag{9}$$

where $(.)^T$ is the transpose operator.

The new set of base functions $S^m_{\alpha}(\theta_{\mathrm{IPP}},,\xi_{\mathrm{IPP}})$ is called Slepian functions, here. Each Slepian function is identified by two indices. First index is m indicating order of the SH. The second index, α, is called in this work the

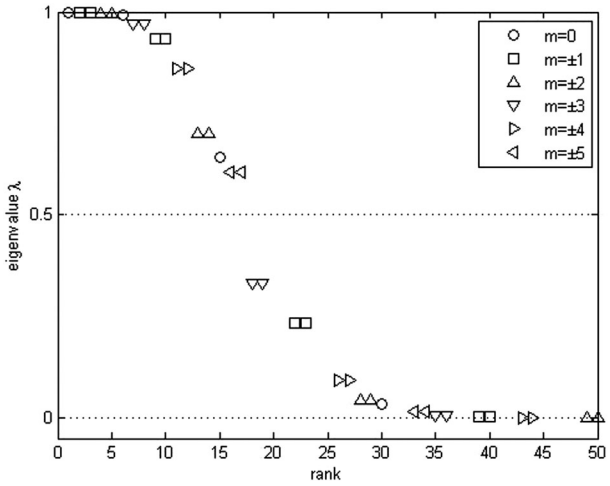

Figure 1. Eigenvalues of $\mathbf{D}^m$ for $0 \le m \le 5$ in the spherical cap of this research (vertical and horizontal axes are eigenvalues and rank, respectively).

degree of Slepian functions; however, it cannot be directly compared to the degree of SHs or the concept of degree in a polynomial as well. Equation (9) precisely transforms harmonic basis of the fixed order m to the corresponding Slepian one [*Albertella et al.*, 1999]. It shows that a Slepian function of degree α is a linear combination of the surface SHs of the same order m. Correspondingly, matrix of eigenvectors can be used to transform the coefficients of the Slepian functions.

$$\Psi_\alpha^m = \sum_{l=|m|}^{K} \left(\mathbf{a}_l^m\right)^T \psi_{lm} \quad , \{|m| \le \alpha \le K\} \tag{10}$$

Ψ_α^m indicates the coefficients of the new (Slepian) base functions. In this paper Slepian functions and their coefficients are derived from GIMs using equations (8)–(10). Finally, by the Slepian approach, VTEC is reconstructed by

$$\mathrm{VTEC}_{\mathrm{Slep}}(\theta_{\mathrm{IPP}}, \xi_{\mathrm{IPP}}) = \sum_{m=-M}^{M} \sum_{\alpha=1}^{N} \Psi_\alpha^m S_\alpha^m (\theta_{\mathrm{IPP}}, \xi_{\mathrm{IPP}}) \tag{11}$$

Here M and N are maximum order and degree of Slepian functions.

2.3. Model Analysis

Generally, the concept of resolution is an efficient way to characterize miss-modeling in a discrete inverse problem ($\mathbf{d} = \mathbf{Am}$). In this approach, it is possible to see how closely the inverse solution matches a given model, assuming that there are no errors in the data. Beginning with an arbitrary model $\mathbf{m}$, by multiplying $\mathbf{A}$ times, a corresponding data vector $\mathbf{d}$ can be found. Then, multiply regularized inverse of $\mathbf{A}(\mathbf{A}_\dagger)$ times $\mathbf{d}$, an inverse solution ($\mathbf{m}_\dagger$) is derived,

$$\mathbf{m}_\dagger = \mathbf{A}_\dagger \mathbf{Am} \tag{12}$$

The model space resolution matrix, $\mathbf{R}_m$, is then defined as

$$\mathbf{R}_m = \mathbf{A}_\dagger \mathbf{A} \tag{13a}$$

By using the theorem of singular value decomposition [*Aster et al*. 2011],

$$\mathbf{R}_m = \mathbf{V}_p \mathbf{V}_p^T \tag{13b}$$

Here p is the number of singular values which are effectively nonzero and the vector $\mathbf{V}$ is the right singular vector of the design matrix $\mathbf{A}$. If the model null space is trivial, $\mathbf{R}_m$ is an identity matrix. But if rank $(\mathbf{A}) = p < n$, the model space resolution matrix is instead asymmetric matrix describing how the inverse solution smears out the original model, $\mathbf{m}$, into a recovered model, $\mathbf{m}_\dagger$ [*Aster et al*. 2011]. In other words, if any of the diagonal entries of this matrix are close to zero, then the corresponding model parameters will be poorly resolved. The model resolution matrix does not depend on specific data values but is an exclusive property of the matrix $\mathbf{A}$. Thus, it can be calculated during the design phase of an experiment to assess expected resolution for a model. An optimal design for the geometry of the model results in a resolution matrix which is close to identity [*Aster et al*. 2011]. Based on this idea, the concept of the model space resolution matrix is used to support the outputs of this research.

3. Numerical Results

Slepian functions as well as the corresponding coefficients are computed here for the northern polar region. It is carried out by the method outlined in sections 2.1 and 2.2. To support the proposed method, SH and

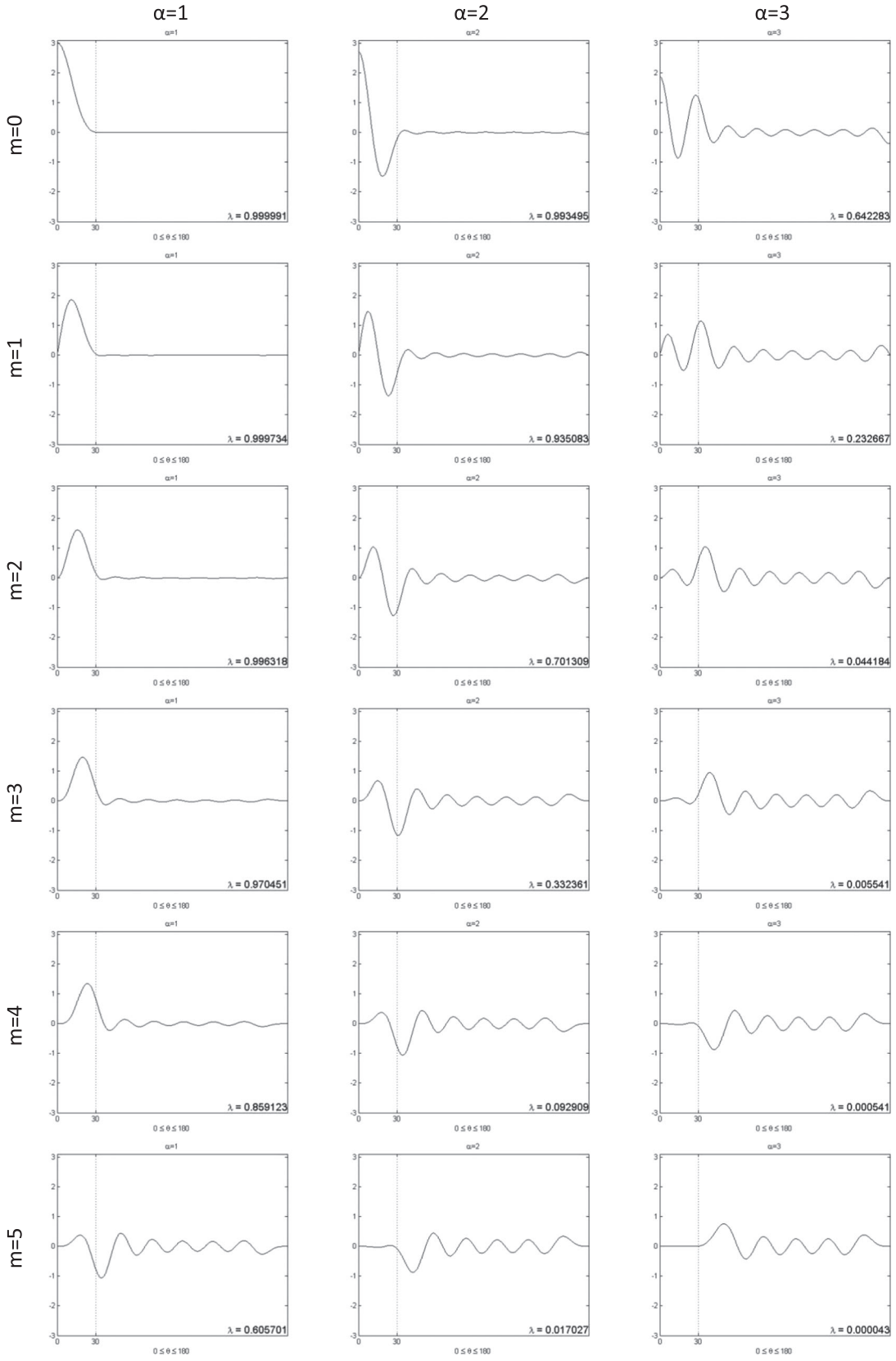

Figure 2. Eigenfunctions of the first three largest eigenvalues of $\mathbf{D}^m$, for $0 \leq m \leq 5$ (vertical and horizontal axes are value of eigenfunction and colatitudinal, respectively).

Table 1. The Number of Slepian Functions Adopted for Modification of the IGS GIMs

	Values					
m	0	±1	±2	±3	±4	±5
α	1, 2, 3	1, 2	1, 2	1	1	1

Slepian resolution matrices are firstly derived. Resolution matrices are used to determine contribution of each model's bias in VTEC estimating process. It will be checked afterward by obtaining the VTECs and a comparison to their estimates directly derived from the dual-frequency GPS measurements.

3.1. Slepian Functions and Their Coefficients

To analyze the accuracy of the proposed method, a spherical cap, with the cap size of 30° at the North Pole, has been taken into account. The maximal degree and order of SH coefficients in the IGS GIM products is 15. Here the adopted maximal modeling degree is assumed the same.

To define the new base functions, $\mathbf{D}^m$ should be computed first. Eigenvalues of this matrix are then computed for $m \in \{0, 1, \ldots, 15\}$. Figure 1 illustrates the computed eigenvalues for $m \leq 5$. For $m > 5$, eigenvalues are close to zero. Therefore, they are not given in this figure. Estimated eigenvalues and eigenvectors reconstruct the matrix $\mathbf{D}^m$ in the spectral domain. Larger eigenvalues contribute more in the spectral decomposition of this matrix. It emphasizes on the role of larger eigenvalues compared to smaller ones in constructing the new base functions (see equation (9)).

Using equation (9), the new base functions and eigenfunctions are computed for each above eigenvalue. Figure 2 illustrates the eigenfunctions which correspond to the three largest eigenvalues of $\mathbf{D}^m$, for $0 \leq m \leq 5$. It is obviously seen that the computed eigenfunctions are the most optimally concentrated ones. Colatitudinal dependency of these functions is also seen in this figure.

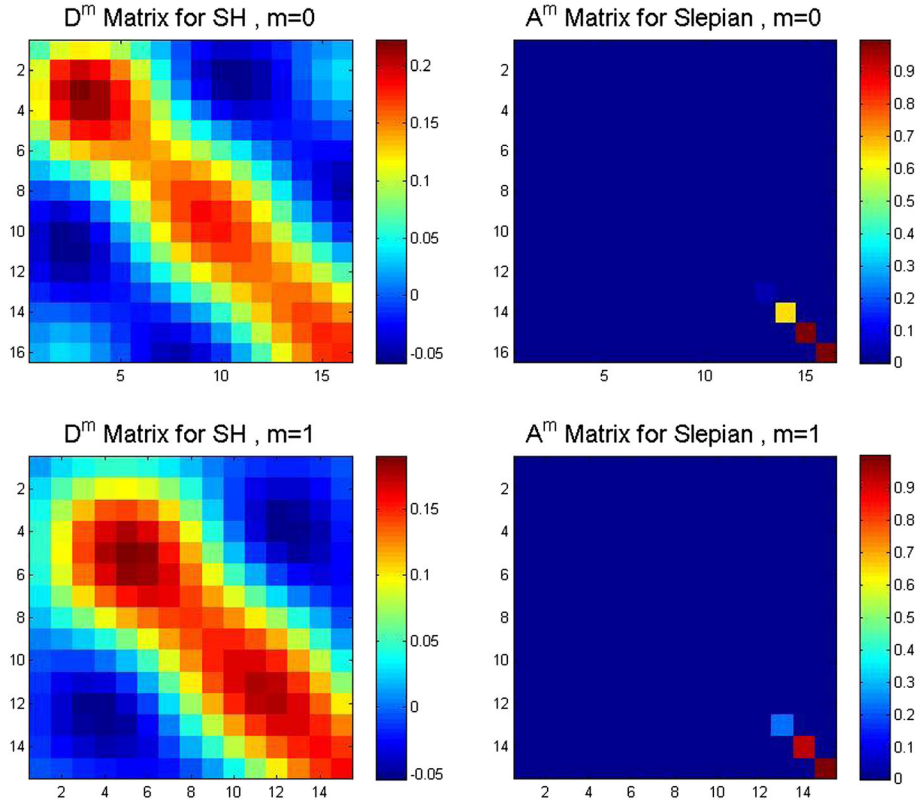

Figure 3. Graphical illustration of the design matrices $\mathbf{D}^m$ and $\mathbf{A}^m$ ($m = 0, 1$).

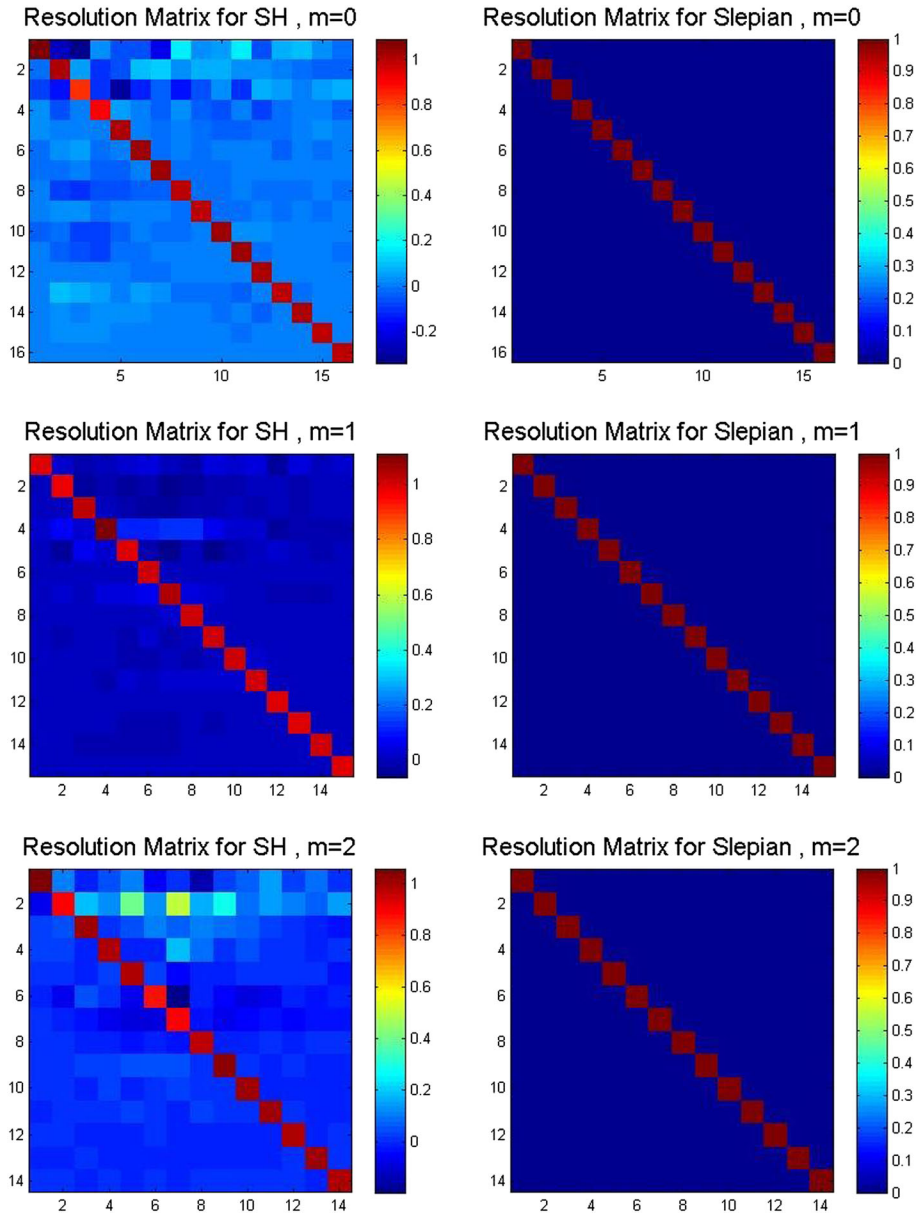

Figure 4. Fixed order resolution matrices for the SH and Slepian basis functions.

According to Figures 1 and 2, the colatitudinal dependency of the eigenfunctions is more prominent for the larger eigenvalues of $\mathbf{D}^m$. Therefore, GIMs have been modified using the eigenfunctions whose eigenvalues conform to the Shannon number rule [*Slepian and Sonnenblick*, 1965]. In other words, the Shannon number is used as a means for selecting the optimum number of the Slepian base functions in this process. For example, the first three eigenfunctions are used when $m = 0$. Table 1 provides the corresponding details.

The role of Shannon number in reconstructing the Slepian design matrix $\mathbf{A}^m$ from the corresponding SH, i.e., $\mathbf{D}^m$, is graphically illustrated in Figure 3.

3.2. The SH and Slepian Resolution Matrices

In the discrete inverse problem of modeling VTEC, the model geometry is constrained by the type and number of the adopted basis functions. Using SHs and Slepian functions for constructing $\mathbf{D}^m$ and $\mathbf{A}^m$, model space resolution matrices have been computed for the study area of this research. Figure 4 illustrates the corresponding results for $m = 0,\ 1,$ and 2, respectively.

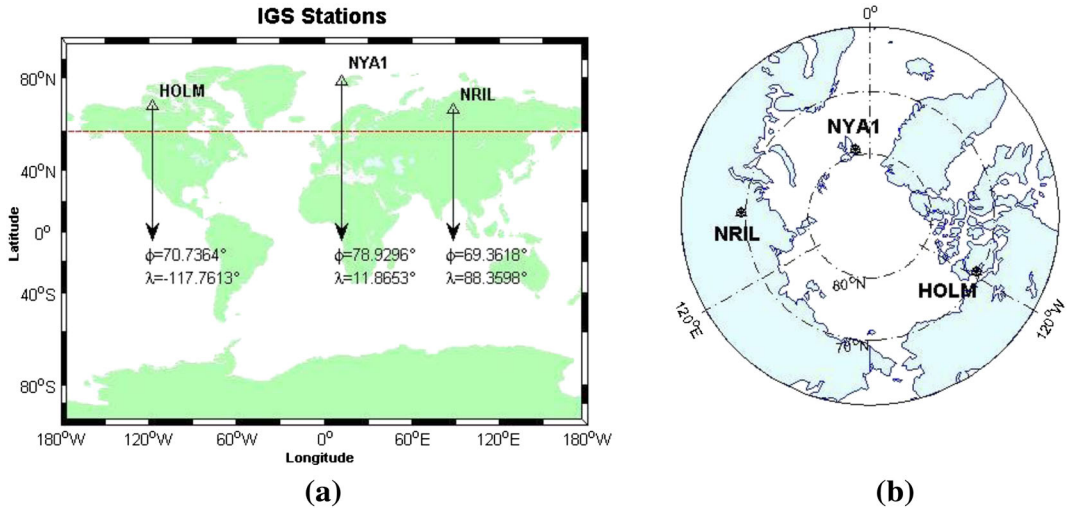

Figure 5. Distribution of the IGS stations used to compare the Slepian and SH models in (left) Miller and (right) stereographic projection systems.

According to the obtained results, model space resolution matrices are closer to identity for the Slepian approach of this research. This implies that VTECs computed by the modified GIMs are expected to be less biased in comparison to VTECs derived from SH models.

3.3. Ionosphere Modeling Using Slepian Functions

Observation files of three IGS stations located in the northern polar cap are used for analyzing the accuracy of ionospheric models in this research. The accuracy of the modified model is also compared to the accuracy of the IGS GIM products.

The spatial distribution of the test stations provides a reasonable coverage for analyzing the accuracy of models within the study area of this research. This distribution is given in Figure 5. The GPS stations of this study are located in Russia (NRIL), Northern Europe (NYA1), and Canada.

In order to assess the Ionospheric modeling by the proposed method, different days with different solar activities are used. According to that, GPS measurements of 15 successive days (from day of year (DOY) 69 to DOY 83 in the year 2013) have been used. The corresponding receiver-independent exchange observation files have been downloaded from the Scripps Orbit and Permanent Array Center (SOPAC) data archive of the IGS. VTECs are computed by the dual-frequency measurements of the data for each satellite and in all measurement epochs ($VTEC_{GPS}$). VTECs are estimated using the pseudo-ranges which are smoothed by the GPS carrier phase measurements. Observations are firstly preprocessed using the Bernese GPS software (the cutoff angle is considered 15°). At this step, not only the cycle slips are detected and repaired but also outlier measurements (or noisy raw observations) have been removed [*Wu et al*. 2010]. Next the smoothed pseudo-ranges are computed using equations below:

$$\left.\begin{aligned}\widetilde{P}_1(t) &= \phi_1(t) + \overline{P}_1 - \overline{\phi}_1 + \frac{2f_2^2}{f_1^2 - f_2^2}\left(\left(\phi_1(t) - \overline{\phi}_1\right) - \left(\phi_2(t) - \overline{\phi}_2\right)\right)\\ \widetilde{P}_2(t) &= \phi_2(t) + \overline{P}_2 - \overline{\phi}_2 + \frac{2f_1^2}{f_1^2 - f_2^2}\left(\left(\phi_1(t) - \overline{\phi}_1\right) - \left(\phi_2(t) - \overline{\phi}_2\right)\right)\end{aligned}\right\} \Rightarrow \mathrm{VTEC}(t) = \frac{f_1^2 f_2^2\left(\widetilde{P}_2(t) - \widetilde{P}_1(t)\right)cos(\mathrm{EL})}{40.3\left(f_1^2 - f_1^2\right)}, \tag{14}$$

where $\phi_F(t)$ is carrier phase measurements at the epoch t and frequency F. $\overline{P}_F - \overline{\phi}_F$ is the mean difference of all the accepted code and phase measurements in the current observation arc on frequency F. f_1 and f_2 are the carrier frequencies for two different observations (ϕ_1 and ϕ_2), respectively. EL is the elevation angle of the satellite at receiver's position. Differential code biases (DCBs) are considered for computing VTECs from GPS observations. The DCBs of the Center of Orbit Determination in Europe (CODE) from the CODG IONEX are downloaded. Estimated VTECs can be used for analyzing the accuracy and the comparison of ionospheric

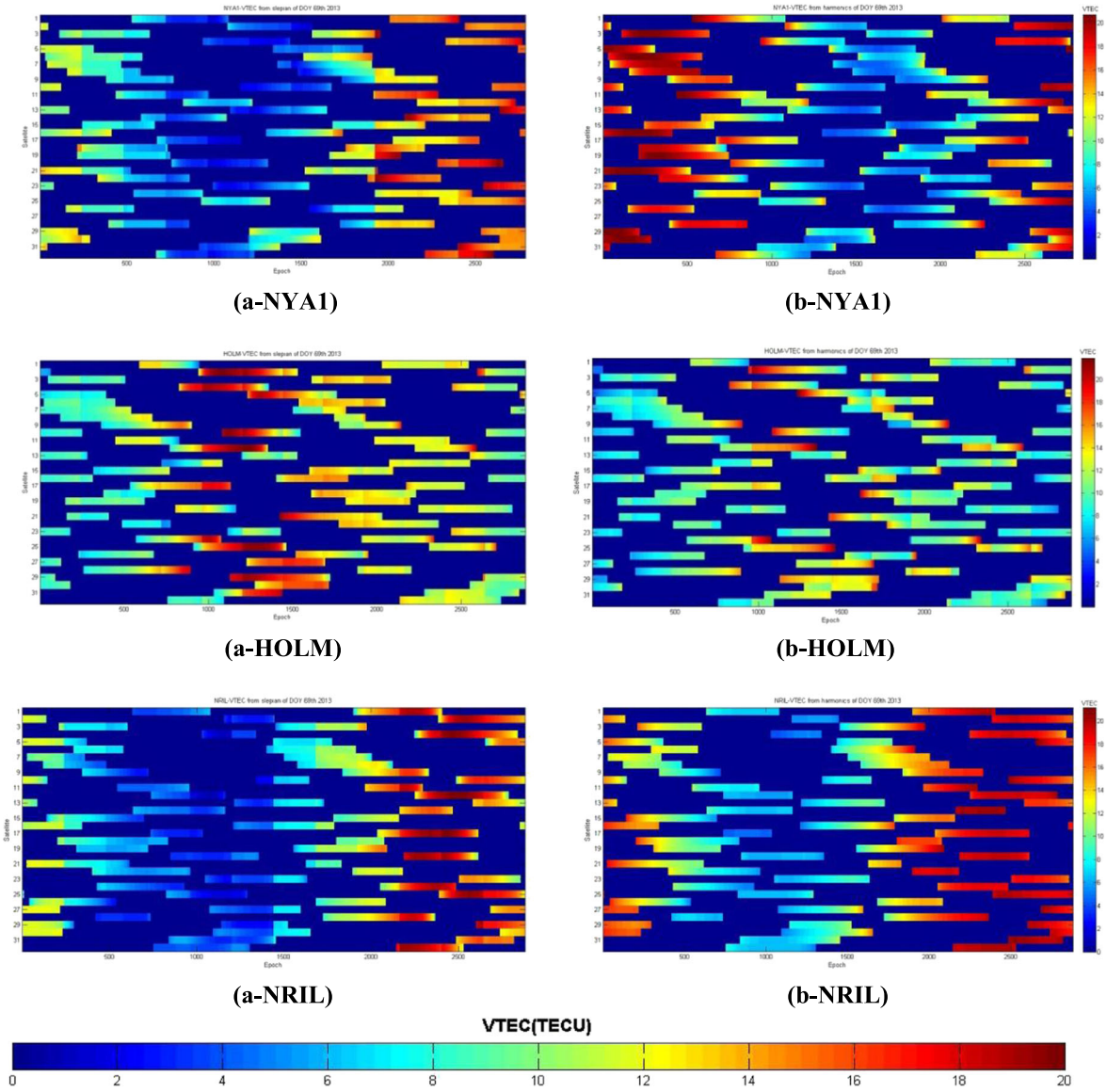

Figure 6. VTECs reconstructed from the modified (a) GIM (Slepian) model and (b) GIM for the DOY 69 of 2013 (vertical and horizontal axes are satellites and 2880 epochs, respectively).

models. In addition to that, coordinates of the IPPs are computed from the GPS observation files. The intersection of the GPS signals with a single-layer shell located at an altitude of 450 km above the Earth is used for this purpose. The IPP coordinates are the inputs of the Slepian and SH models (see equations (1) and (9)).

The IGS SH-based GIMs are the basic data required for the Slepian approach of this research. They are downloaded from the CODE, an IGS associate analysis center, for the time period mentioned above. CODE GIMs include the SH coefficients during a day at 2 h intervals ($VTEC_{SH}$). As the result, the coefficients of the Slepian base functions have been computed in 2 h intervals too. Equation (10) is used for this purpose. VTECs have been reconstructed using equation (11) ($VTEC_{Slep}$). Figure 6 illustrates the obtained results for the DOY 69 of the year 2013.

Differences of the VTEC which is computed by GPS measurements ($VTEC_{GPS}$) and the modeled ones are used as a benchmark for analyzing the accuracy of models (i.e., $dVTEC_{GPS\,-\,SH} = VTEC_{GPS} - VTEC_{SH}$ and $dVTEC_{GPS\,-\,Slep} = VTEC_{GPS} - VTEC_{Slep}$). Here two methods are used for the assessment of the obtained results.

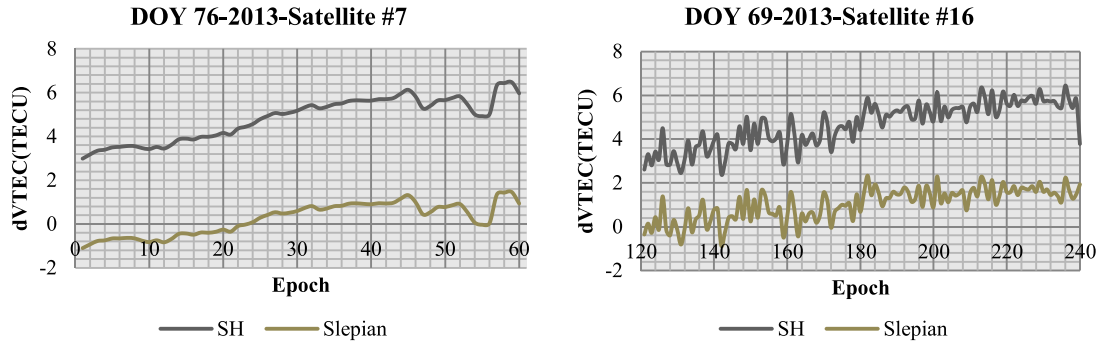

Figure 7. dVTECs for two arbitrary satellites.

In the first approach, differences are computed and analyzed for each satellite, separately. Differences are computed for 60 and 120 successive epochs of measurements to GPS satellites 7 and 16, respectively. Figure 7 illustrates the obtained results. Based on this figure, the model biases ($dVTEC_{GPS-SH}$ and $dVTEC_{GPS-Slep}$) are negative in some of the measurement epochs. Moreover, the epoch-wise comparison of the estimated biases illustrates that the (Slepian) modified model performs more accurately than the SH one.

As the second approach, the mean of the absolute values of dVTECs are computed for satellites in sight at each measurement epoch ($\overline{dVTEC}$). Figure 8 illustrates the obtained results.

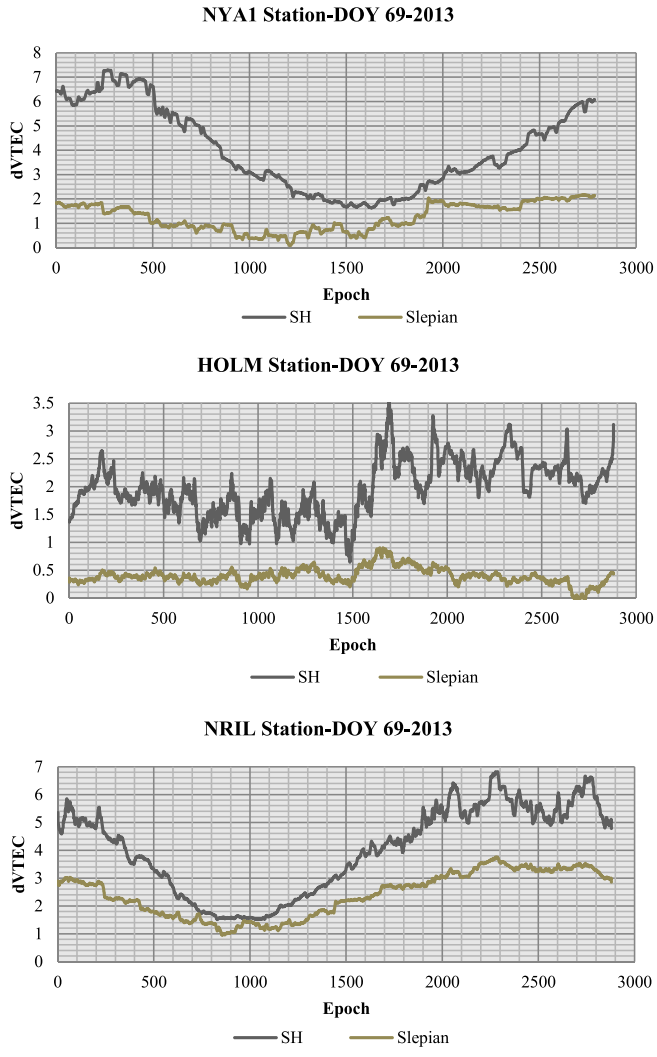

Figure 8. $\overline{dVTEC}$s which are computed for the Slepian and SH models for the DOY 69 of the year 2013.

Nonzero elements in the $\overline{dVTEC}$ time series emphasize on the biaseness of both models. Again, the existing bias of the modified model is obviously smaller than the SH model. The existing smaller bias in the former results suggests an improved performance of the approach of this study for ionosphere modeling in polar regions. To explore pros and cons of the Slepian modification in further details, the daily means of the $\overline{dVTEC}$ time series have been computed and compared to each other, too. This measure can provide a means for the direct comparison of the obtained results spatially and temporally. Figure 9 reports on the obtained results. Again, the improved performance of the Slepian approach in modeling ionosphere is clearly seen in the corresponding results. The existing differences between estimated averages of the daily $\overline{dVTEC}$s for the Slepian modified and SH models roughly suggest an improvement of about 1 to 2 total electron content unit (TECU) in the accuracy of the model using the

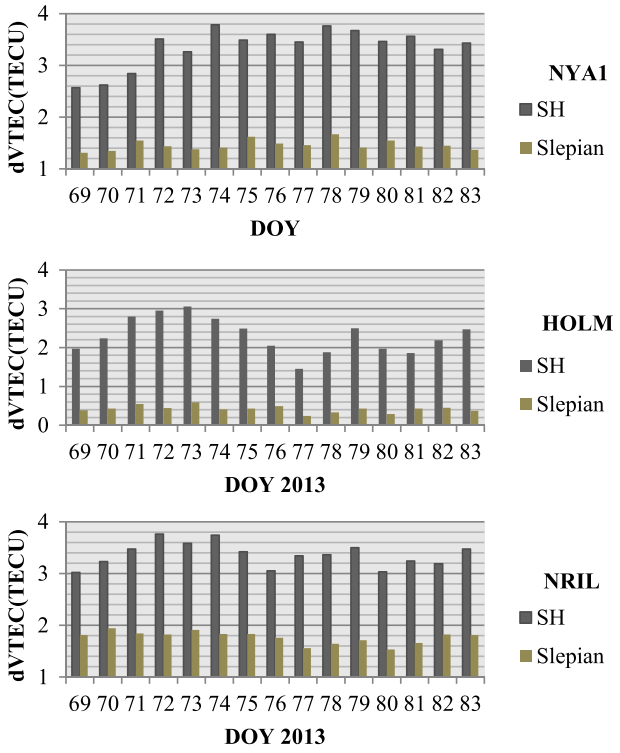

Figure 9. Daily averages of $\overline{\text{dVTEC}}$s for the time interval from DOY 69 to DOY 83.

Slepian approach of this research. This improvement is also confirmed through the comparison of the SH and Slepian model resolution matrices provided in section 3.2.

4. Conclusion

A modification method is proposed for improving the accuracy of CODE GIMs in polar regions. The proposed method is based on the spatiospectral concentration of the base functions. The accuracy of this method is then analyzed using the model resolution matrices as well as the GPS measurements of 15 successive days.

According to the obtained results, the application of Slepian basis functions which maximizes the concentration of the sought signal not only improves the resolution of the modified model but also discards some of the nuisance parameters that contribute in the miss-modeling process when SHs are used. In other words, the comparison of resolution matrices suggests that the SH approach for modeling VTEC suffers from an overparameterization, that is, balanced through the modification method of this research.

The accuracy of the modified model has been compared to CODE GIM products. Although both of the modified (Slepian) and the CODE models are biased, the accuracy of the modified model is about 1 to 2 TECU better than the global ionosphere products.

Acknowledgments
5The GPS data used in this research are available at Scripps Orbit and Permanent Array Center (SOPAC) data archive of the IGS (website: http://sopac.ucsd.edu/cgi-bin/dbDataBySite.cgi), and the IGS GIMs are from the Center of Orbit Determination in Europe (CODE), an analysis center of IGS (website: ftp://ftp.unibe.ch/aiub/CODE).

References

Aarons, J. (1982), Global morphology of ionospheric scintillation, *Proc. IEEE*, *70*, 360–378.
Aarons, J. (1993), The longitudinal morphology of equatorial F-layer irregularities relevant to their occurrence, *Space Sci. Rev.*, *63*(3–4), 209–243.
Albertella, A., F. Sansò, and N. Sneeuw (1999), Band-limited functions on a bounded spherical domain: The Slepian problem on the sphere, *J. Geod.*, *73*, 436–447.
Aster, R. C., B. Borchers, and C. Thurber (2011), *Parameter Estimation and Inverse Problems*, vol. 90, Elsevier Acad. Press.
Basu, S., K. M. Groves, S. Basu, and P. J. Sultan (2002), Specification and forecasting of scintillations in communication/navigation links: Current status and future plans, *J. Atmos. Sol. Terr. Phys.*, *64*, 1745–1754.
Dow, J. M., R. E. Neilan, and C. Rizos (2009), The International GNSS Service in a changing landscape of Global Navigation Satellite Systems, *J. Geod.*, *83*, 191–198, doi:10.1007/s00190-008-0300-3.
Edmonds, A. R. (1996), *Angular Momentum in Quantum Mechanics*, Princeton Univ. Press, Princeton, N. J.

Fremouw, E. J., and J. A. Secan (1984), Modeling and scientific application of scintillation results, *Radio Sci.*, *19*(3), 687–694, doi:10.1029/RS019i003p00687.
García-Rigo, A., M. Hernández-Pajares, and R. Orús-Pérez (2014), UPC contributions to GNSS monitoring of ionosphere in the frame of the IGS Iono-WG, IGS Workshop 2014, June 23–27, Pasadena, Calif.
Georgiadiou, Y. (1994), *Modeling the Ionosphere for an Active Control Network of GPS Station*, *LGR- series (7)*, Delft Geodetic Computing Centre, Delft.
GhoddousiFard, R., P. Héroux, D. Danskin, and D. Boteler (2011), Developing a GPS TEC mapping service over Canada, *Space Weather*, *9*, S06D11, doi:10.1029/2010SW000621.
Hunsucker, R. D., and J. K. Hargreaves (2003), *The High-Latitude Ionosphere and Its Effects on Radio Propagation*, Cambridge Univ. Press, New York.
Jin, S. G., E. Cardellach, and F. Xie (2014), *GNSS Remote Sensing: Theory, Methods and Applications*, 276 pp., Springer, Netherlands.
Klobuchar, J. A. (1987), Ionospheric time delay algorithm for single-frequency GPS users, *IEEE Trans. Aerosp. Electron. Syst.*, *AES-23*(3), 325–331.
Komjathy, A. (1997), Global ionospheric total electron content mapping using the Global Positioning System, Dissertation, Univ. of New Brunswick.
Kunitsyn, V., and E. Tereshchenko (2003), *Ionospheric Tomography*, Springer, New York.
Landau, H. J., and H. O. Pollak (1961), Prolate spheroidal wave-functions, Fourier analysis and uncertainty II, *Bell Syst. Tech. J.*, *40*(1), 65–84.
Landau, H. J., and H. O. Pollak (1962), Prolate spheroidal wave functions, Fourier analysis, and uncertainty III, *Bell Syst. Tech. J.*, *41*, 1295–1336.
Liu, J., Z. Wang, H. Zhang, and W. Zhu (2008), Comparison and consistency research of regional ionospheric TEC models based on GPS measurements, *Geomat Inf Sci Wuhan Univ.*, *33*(5), 479–483.
Liu, J., R. Chen, Z. Wang, and H. Zhang (2011), Spherical cap harmonic model for mapping and predicting regional TEC, *GPS Solut.*, *15*(2), 109–119.
Liu, J., R. Chen, J. An, Z. Wang, and J. Hyyppä (2014a), Spherical cap harmonic analysis of the Arctic ionospheric TEC for one solar cycle, *J Geophys Res Space Physics*, *119*, 601–619, doi:10.1002/2013JA019501.
Liu, J., R. Chen, Z. Wang, J. An, and J. Hyyppä (2014b), Long-term prediction of the arctic ionospheric TEC based on time-varying periodograms, *PLoS One*, *9*(11), e111497, doi:10.1371/journal.pone.0111497.
Luhr, H., and C. Xiong (2010), IRI-2007 model overestimates electron density during the 23/24 solar minimum, *Geophys. Res. Lett.*, *37*, L23101, doi:10.1029/2010GL045430.
Messiah, A. (2000), *Quantum Mechanics*, Dover, New York.
Parkinson, B. W., and J. J. Spilker (1996), *Global Positioning System: Theory and Applications*, vol. I and II, Am. Inst. Aeronaut. Astronaut., Washington D. C.
Rodger, A. S., and A. C. Graham (1996), Diurnal and seasonal occurrence of polar patches, *Ann. Geophys.*, *14*, 533–537.
Schaer, S. (1999), Mapping and predicting the Earth's ionosphere using the Global Positioning System, Dissertation, Univ. of Bern.
Schaer, S., W. Gurtner, and J. Feltens (1998), IONEX: The ionosphere map exchange format version 1. Astronomical Inst., Univ. of Berne, Switzerland and Darmstadt, Germany. [Available at ftp://igscb.jpl.nasa.gov/igscb/data/format/ionex1.pdf, Accessed 19 June 2009.]
Seeber, G. (2003), *Satellite Geodesy: Foundations, Methods, and Applications*, 2nd ed., Walter de Gruyter Inc.
Simons, F. J. (2010), Slepian functions and their use in signal estimation and spectral analysis, in *Handbook of Geomathematics*, edited by T. Sonar, Z. M. Nashed and W. Freeden, pp. 891–923, Springer, Germany, doi:10.1007/978-3-642-01546-5_30.
Simons, F. J., F. A. Dahlen, and M. A. Wieczorek (2006), Spatiospectral concentration on a sphere, *SIAM Rev.*, *48*, 504–536.
Simons, F. J., J. C. Hawthorne, and C. D. Beggan (2009), Efficient analysis and representation of geophysical processes using localized spherical basis functions, in *Wavelets XIII*, vol. 7446, edited by V. K. Goyal, M. Papadakis, and D. Van De Ville, SPIE, San Diego, Calif., 74460G15.
Skone, S. (1998), Wide area ionosphere grid modeling in the auroral region PhD thesis, published as report No. 21023, Dep. Geomatics Eng., Univ. of Calgary, Canada.
Skone, S. (2009), *Atmospheric Effects on Satellite Navigation System, ENGO633 Course Notes*, Dep. Geomatics Eng., Univ. Calgary, Canada.
Skone, S., G. Lachapell, D. Yao, W. Yu, and R. Watson (2005), Investigating the impact of ionospheric scintillation using a GPS software receiver, Presented at the ION GNSS 2005 Conference, Long Beach, Calif.
Slepian, D. (1976), On bandwidth, *Proc. IEEE*, *64*(3), 292–300, doi:10.1109/PROC.1976.10110.
Slepian, D. (1978), Prolate spheroidal wave functions, Fourier analysis and uncertainty V: The discrete case, *Bell Syst. Tech. J.*, *57*(2), 1371–1430.
Slepian, D. (1983), Some comments on Fourier analysis, uncertainty and modeling, *SIAM Rev.*, *25*, 379–393.
Slepian, D., and E. Sonnenblick (1965), Eigenvalues associated with prolate spheroidal wave functions of zero order, *Bell Syst. Tech. J.*, *44*, 1745–1759.
Slepian, D., and H. O. Pollak (1961), Prolate spheroidal wave functions, Fourier analysis, and uncertainty I, *Bell Syst. Tech. J.*, *40*(1), 43–63.
Werink, A. W., J. A. Secan, and E. J. Fremouw (2003), Ionospheric irregularities and scintillation, *Adv. Space Res.*, *31*(4), 1750–1757.
Wu, Y., S. G. Jin, Z. M. Wang, and J. B. Liu (2010), Cycle slip detection using multi-frequency GPS carrier phase observations: A simulation study, *Adv. Space Res.*, *46*(2), 144–149.